CI&CEQ
Chemical Industry & Chemical Engineering Quarterly

Available online at
Association of the Chemical Engineers of Serbia AChE
www.ache.org.rs/CICEQ

Chem. Ind. Chem. Eng. Q. 29 (3) 189–200 (2023) CI&CEQ

AMARÍLIS SEVERINO E SOUZA[1]
THIAGO CÉSAR DE SOUZA PINTO[2]
ALFREDO MOISÉS SARKIS[3]
THIAGO FAGGION DE PÁDUA[1]
RODRIGO BÉTTEGA[1]

[1]Federal University of São Carlos, Department of Chemical Engineering, Drying Center of Pastes, Suspensions, and Seeds, São Carlos, SP, Brazil

[2]Mineral Development Center – CDM/Vale, Santa Luzia, MG, Brazil

[3]Instituto Tecnológico Vale – ITV, Santa Luzia, MG, Brazil

SCIENTIFIC PAPER

UDC 622.785:66.047

ENERGY ANALYSIS OF THE CONVECTIVE DRYING OF IRON ORE FINES

Article Highlights

- Characterization of iron ore fines according to IMSBC code
- Handling and drying of wet agglomerates of iron ore fines in a fixed bed
- Each air condition was associated with an optimal solids load that minimized the SEC
- Drying at the identified optimal condition resulted in the highest energy efficiency

Abstract

Drying operations in iron ore processing plants have a particularly high energy demand due to the massive solid flow rates employed in this industry. A 3^3 full-factorial design was applied to investigate the effects of air temperature, airflow velocity, and solids load on the drying time and the specific energy consumption (SEC) of the convective drying of iron ore fines in a fixed bed. The results demonstrated that each drying air condition was associated with an optimal solids load that minimized the SEC. A load of 73 g (bed height of about 0.8 cm) was identified and validated as the optimal condition in terms of energy consumption for the configuration with the highest air temperature (90 °C) and airflow velocity (4.5 m/s). This condition resulted in a drying time of 29.0 s and a corresponding SEC of 12.8 MJ/kg to reduce the moisture from 0.11 kg water/kg dry solids to a target of 0.05 kg water/kg dry solids. Identifying the optimum values for the process variables should assist in designing and operating energy-efficient convective dryers for iron ore fines.

Keywords: iron ore agglomerates, transportable moisture limit, energy consumption, drying efficiency, pellet feed.

An important step in the processing of iron ore is the removal of moisture. The grinding and separation processes of mineral species are usually carried out using wet routes, so there is a subsequent need to remove water from concentrates before sending the ore to direct reduction, pelletizing, or exportation [1–3]. Even after the dewatering processes, rain and poor conditions at the storage yards can increase the amount of water in the ore. These problems are detrimental for direct shipping ores because a high moisture level increases the freight cost and decreases the profit since the price of the sold ore is assessed on a dry basis. Another issue is that, before shipping, the iron ore must comply with the maximum moisture level established by the International Maritime Organization (IMO) for the safe transport of bulk materials in ships, known as the Transportable Moisture Limit (TML) [4,5].

Iron ore fines are classified as Group A cargo according to the IMSBC (International Maritime Solids Bulk Cargoes) Code [5]. It means that if the moisture content of this material is above the TML, the wet mineral cargo is subject to liquefaction. When ore liquefaction occurs in the cargo hold, the ship can progressively lose its stability due to cargo movement and may capsize and sink. Consequently, if the material does not comply with the TML value, the cargo is rejected, and the product remains in the storage yards,

Correspondence: A. Severino E Souza, Federal University of São Carlos, Department of Chemical Engineering, Drying Center of Pastes, Suspensions, and Seeds, São Carlos, SP, Brazil.
E-mail: amarilis.sev@gmail.com
Paper received: 8 February, 2022
Paper revised: 25 May, 2022
Paper accepted: 11 October, 2022

https://doi.org/10.2298/CICEQ220208026S

causing economic losses for the mining company and difficulties in handling procedures, affecting the entire production chain. Therefore, dewatering and drying systems are important for commercializing and transporting this ore.

The TML value can vary widely according to the characteristics of the ore. Moreira *et al.* [6] investigated the variation of TML for iron ore according to particle size distribution. They concluded that the addition of fine particles could increase the TML. Munro and Mohajerani [4] and Ferreira *et al.* [7] determined the TML for samples with various size distributions, iron contents, and mineralogical compositions. The results of these studies covered TML values from 8.00% to 16.80% and from 7.69% to 14.95%, respectively, representing considerable ranges in terms of moisture. Usually, when the mechanical removal of water from a specific variety of iron ore using hydrocyclones [8], thickeners [9], filters [10,11], and vacuum filters [12,13] is not sufficient to meet the TML standard, or when layout or process conditions do not permit installation of these systems, thermal drying becomes necessary.

Since thermal drying requires hot air, the process is expensive for ore processing plants in terms of fuel consumption, equipment, dust abatement, and greenhouse gas generation. On the other hand, convective drying is one of the industrial processes with the highest energy demand [14,15] because it provides the thermal energy necessary to vaporize moisture. Consequently, the energy required for drying massive amounts of ore under severe air velocity and temperature conditions is one of the main challenges for employing and maintaining convective drying in iron ore processing plants [16]. For example, a temperature of more than 1000 °C and an airflow of 4.6 t/h were used to dry an iron ore flow of 4.0 t/h at an initial moisture level of 19% (wet basis) [17]. Considering this commodity's relatively low unit price (U$168 per dry metric ton of 62.5% Fe ore in 2021 [18]), the drying air conditions, and the process's scale, drying operations incur high costs for the mining industry. Therefore, studies that offer strategies for efficient energy use are of paramount interest to this sector [19].

Although drying processes represent a considerable challenge for the mining industry, the the existing work in this area is scarce [19,20]. Considering iron ore drying, the literature focuses on pellets [21–25], while work regarding iron ore fines is rare. In drying iron ore fines, Namkung and Cho [26] determined some fluid dynamic aspects of a pneumatic dryer operating with iron ore particles with diameters ranging. For an initial moisture content of 6.95% (wet basis), it was observed that the degree of particle drying increased from 48.6% to 82.5% with an increase in the air temperature from 100 °C to 400 °C. Souza Pinto *et al.* [27] investigated the characteristics and drying kinetics of iron ore pellet and sinter feed. This study showed that for a drying operation using a fixed bed with an air temperature of 400 °C, moisture removal decreased by around 60% when the operation involved the final drying stage (falling rate period). This result indicated potential energy savings and cost reductions for drying operations occurring within the initial drying period (constant rate). However, no further investigation was performed on the energy aspects of iron ore fines drying operations.

Knowledge about energy consumption is important for a better understanding of the drying processes. The thermal energy consumption of hot air drying operations in a fixed bed is related to the drying air conditions and the solids load. The few studies that have investigated the effect of the solids load on the specific energy consumption of drying operations [28,29] have reported that increasing the solids load resulted in lower energy consumption. Nevertheless, in these experimental studies, no analysis was performed to investigate if there was a limit to this trend. Since the further increase of the solids loads also leads to less energy being absorbed per unit mass, the evaporation rates can drop, and the drying time can rise to the point of increasing the energy consumption of the process. Therefore, additional studies are still required to investigate the behavior of the energy consumption of drying processes in fixed beds according to the solids load.

The objective of the present work was to analyze the drying kinetics and energy consumption for the convective drying of iron ore fines in a fixed bed. To this end, a 3^3 full-factorial design and a statistical analysis using response surface methodology were employed to investigate the effects of the variables solids load, air temperature, and airflow velocity on the responses drying time and specific energy consumption. In addition, the energy performance was evaluated based on energy efficiency, drying efficiency, and specific energy consumption parameters. The aim was to identify operating conditions that could minimize the energy consumption of the drying process.

MATERIALS AND METHODS

Sample characterization and preparation

Dry iron ore samples from Carajás (Pará State, Brazil) were provided by Instituto Tecnológico Vale (ITV-MI). Chemical characterization was performed for a sample fused with lithium tetraborate using an X-ray fluorescence spectrometer (Zetium, Malvern Panalytical). Loss on ignition (LOI) determination was performed using a temperature of 1020 °C for 2 h. The

results obtained were 65.3% Fe, 0.74% SiO_2, 1.10% Al_2O_3, and 3.97% LOI.

The particle size was determined using a Malvern Mastersizer Microplus instrument (Micromeritics). Figure 1 presents the particle size distribution (φ - cumulative; $\Delta\varphi$ - per fraction), showing D_{10} and D_{50} values of around 0.3 μm and 40 μm, respectively. The density of the iron ore was 4.2 g/cm³.

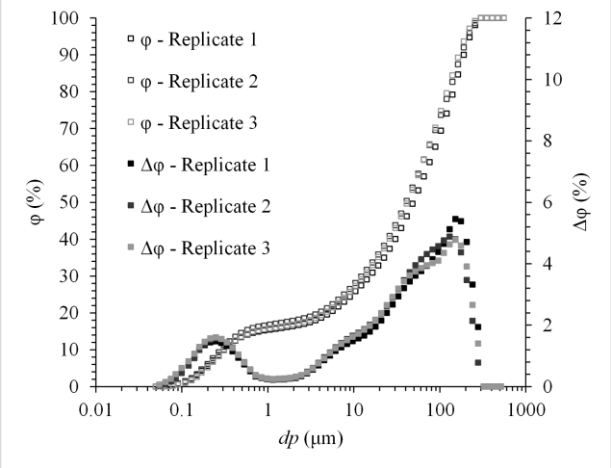

Figure 1. Cumulative particle size distribution of the iron ore fines.

The modal mineralogical composition of the sample was determined by reflected light microscopy (DM750P-Leica). The quantification of hematite minerals, goethite, quartz, silicate, and others, was performed by counting at least 500 grains per polished section. Results showed 72.45% of hematite and 25.28% of goethite. Quartz, silicate, and others were 1.32%, 0.19%, and 0.75%, respectively. Concerning the mineralogical composition (goethite content less than 35%) and the size distribution ($D_{10} \leq 1$ mm and $D_{50} \leq 10$ mm), the sample was classified as Iron Ore Fines according to the IMSBC Code (IMO, 2019), a Group A cargo susceptible to liquefaction if shipped at a moisture content above its TML.

Distilled water was added to portions of 200 g of dry ore until reaching the desired nominal moisture content of 0.11 kg water/kg dry solids (dry basis) to humidify the material [27]. The material was kept in closed plastic bags, at room temperature, for up to 12 h before the tests. Standard deviations for the initial moisture content determined by this method were approximately 0.3%. The dry and humidified ore can be seen in Figure 2. Before the drying assays, the sample of the wet material was extruded through a coarse mesh sieve to standardize the agglomerates that were formed. This procedure maintained the agglomerates with diameters less than 6 mm (sieve opening), and this procedure had no impact on the nominal moisture content of the sample. The formation of agglomerates is a feature of the humidified ore [27,30].

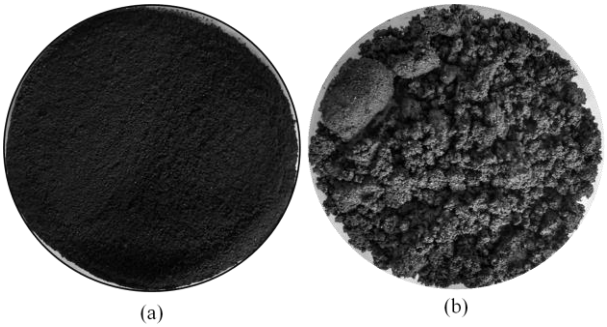

Figure 2. Photographs of the iron ore fines: (a) dry and (b) with a nominal moisture content of 0.11 kg water/kg dry solids, showing agglomeration of wet particles.

Experimental apparatus and procedure

Figure 3 shows the experimental apparatus used in this study. The equipment consisted of a blower with a controlled airflow, an electric heater, and a cylindrical glass drying chamber (7.2 cm inside diameter, 50 cm height). The temperature of the air entering the drying chamber was controlled to within ±1 °C by a temperature controller and remained unchanged at the setpoint during each of the experimental drying assays. The superficial air velocity was measured at the center of the cylindrical drying chamber (Figure 3) using a hot wire anemometer (AK833, Akso) and was adjusted before each assay.

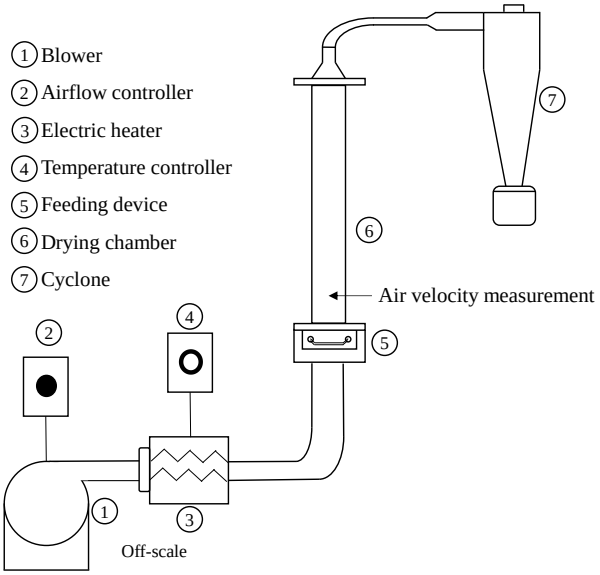

Figure 3. Diagram of experimental apparatus.

A cyclone was installed on the top of the drying chamber to collect entrained fine dust. However, humidification and consequent agglomeration of iron ore fines substantially reduced particle entraining at the analyzed airflow conditions. Therefore, the mass of dust collected by the cyclone was very low (less than 1.5% of the feed), and this portion of the material was neglected when analyzing the drying kinetics.

The feeding device (Figure 4a) consisted of a drawer-like system where a container could be moved

across a fixed base. For loading, the container was entirely removed from the drying chamber, filled with solids, and then inserted back into the system, sealing the chamber and preventing air leakage. The base of the container had a screen that supported the solids and allowed contact of the drying air with the sample. The advantage of the device was the feeding and collecting of the solid agglomerates from the chamber without needing to turn off the air supply, as well as for easy removal and weighing of the whole sample at the end of the drying time. The loaded solids kept a fixed bed configuration during drying (Figure 4b). In order to avoid breakage of the ore agglomerates and consequent dragging of fine particulate material, the fluidized bed condition was not used.

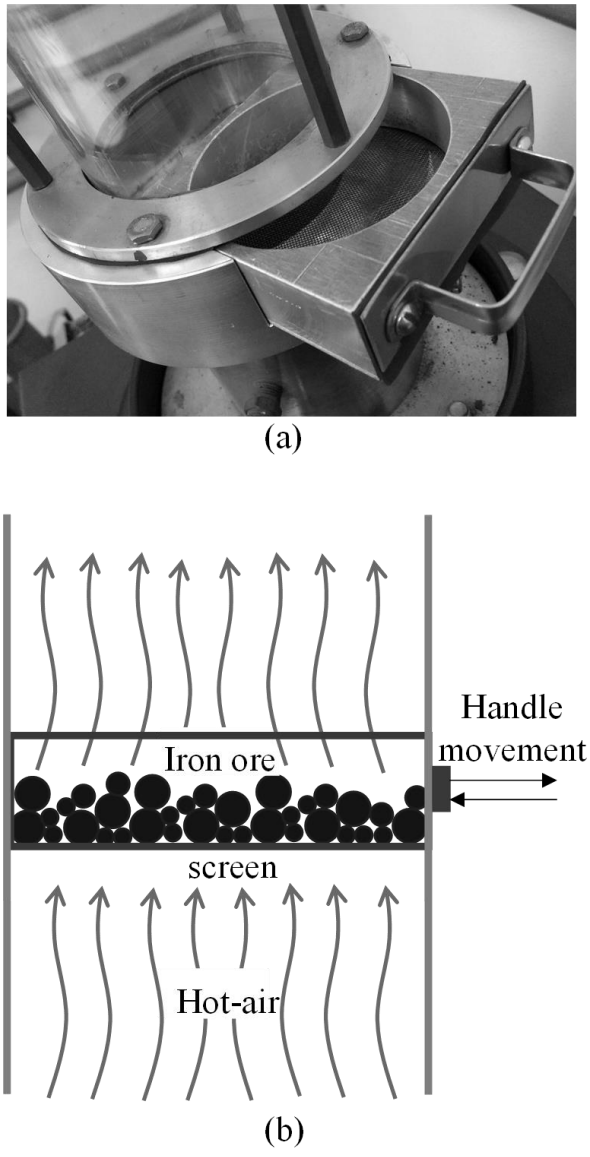

Figure 4. Feeding apparatus (a) photograph, showing attachment of the drawer to the drying chamber, and (b) scheme of air contact with the sample in the drying chamber.

The experimental procedure consisted of setting the operating conditions and stabilizing the system (with the airflow and temperature reaching a steady state), after which the drying chamber was loaded with a mass of wet material at 0.11 kg water/kg dry solid, using the feeding device. At the end of each drying time interval (0 s, 30 s, 60 s, 120 s, 240 s, 360 s, 480 s), the sample was removed from the equipment, weighed, and dried in an oven at a constant temperature of 105 °C. After 24 h, the weight of the sample was measured again to obtain its moisture content [31]. This procedure was performed to obtain the behavior of the moisture content with time.

The process kinetics was described using the dimensionless moisture content:

$$X^*(t) = \frac{X_t - X_{eq}}{X_i - X_{eq}} \quad (1)$$

where X_t is the average moisture content at time t, X_i is the initial moisture content, and X_{eq} is the moisture content at the dynamic equilibrium condition, all on a dry basis. Drying experiments were performed until reaching X_{eq}, which was about 0.003 kg water/kg dry solid.

The temperature of the solids (T_s) was monitored during the drying assays using an infrared thermometer (UT300A, UNI-Trend) with an accuracy of ±2 °C. After removing the sample from the equipment at the end of the drying time, the thermometer was pointed toward the surface of the ore at a distance of about 1 cm. Three temperature readings were performed, and the average value for T_s was employed in the energy analysis to estimate the energy used to heat the solids.

Energy analysis

The usual parameters adopted in the literature were estimated to evaluate the dryer performance [32–34], calculating the energy and drying efficiencies using instantaneous non-cumulative indexes and the specific energy consumption (the total amount of energy necessary to evaporate a unit mass of water). The advantage of using specific energy consumption is that it is an understandable and straightforward measure that considers how efficiently energy is used in the drying process. In addition, this approach has been reported in the literature [32,33] for quantification of the variation of the energy used according to the moisture content of the material.

The energy required to heat the material (Q_m) was calculated using the following equation:

$$Q_m = m_{ws} c_{ps} \left(T_{s,t} - T_{S,i}\right) \quad (2)$$

where m_{ws} is the mass of wet ore, c_{ps} is the specific heat of iron ore, which was considered constant, equal to 620 J kg^{-1} K^{-1} [35], and $T_{s,t}$ and $T_{s,i}$ are the mean temperature of the iron ore at time t and the initial time, respectively.

The energy required to evaporate the water present in the sample (Q_w) was estimated based on the mass of bone-dry ore (m_{ds}) and the latent heat of free water vaporization (ΔH_S):

$$Q_w = \Delta H_S m_{ds} (X_t - X_i) \quad (3)$$

The latent heat of free water vaporization was obtained using Eq. 4 [36]:

$$\Delta H_S = 3168 - 2.4364\ T_S\ (K) \quad (4)$$

The thermal energy supplied to the system (Q) was calculated as follows:

$$Q = \dot{m} c_p (T_f - T_a) \quad (5)$$

where, $\dot{m}$ is the mass flow of air, c_p is the specific heat of air, T_f is the temperature of the drying air, and T_a is the ambient temperature, equal to 25 °C.

The parameters used to analyze the energy performance of the convective dryer were energy efficiency (EE), drying efficiency (DE), and specific energy consumption (SEC) [37]. These parameters were calculated as follows:

$$EE = \frac{Q_w}{Q\ t} \quad (6)$$

$$DE = \frac{Q_w + Q_m}{Q\ t} \quad (7)$$

$$SEC = \frac{Q\ t}{m_{ds}(X_t - X_i)} \quad (8)$$

The heat absorbed by the feeding device and the drying chamber during the assays is process inefficiency, which is accounted for in the energy performance parameters.

Experimental design and statistical analysis

The experimental design technique has been employed to analyze the energy demands and optimize drying process variables for different materials [29,38–40]. This method enables investigation of the effects of the independent variables involved in the process and their interactions, identifying the operating conditions that favor energy savings.

A 3^3 full-factorial design (face-centered composite design) was performed to determine the effect of external conditions on the convective drying of the iron ore fines. The design evaluated the effects of the variables solids load (m_p), air temperature (T_f), and airflow velocity (u_f) on the responses drying time to a 0.05 kg water/kg dry solids moisture content (t_d) and the specific energy consumption required for the sample to attain this moisture value (E_s). A final moisture level of 0.05 kg water/kg dry solids for both t_d and E_s was defined to meet the minimum moisture content desired for iron ore since lower values can lead to high dust generation, product loss, and difficulties in handling the material [41]. Furthermore, this value is above the critical humidity found in tests for other dryers [27] and was used as a reference for drying to occur mainly within the constant rate period. This value is also below the TML usually found for iron ore and hence meets the moisture content required for shipping operations [4,7].

The experimental data of the dimensionless moisture content over time were fitted using a kinetic model (Eq. 9) to obtain the value of t_d [27,42]. The drying time to 0.05 kg water/kg dry solid was then estimated using the equation of the fit. A similar method was employed by Silva *et al.* [43] to estimate the drying time necessary for the sample to achieve a specific moisture level. Finally, the E_s value was calculated for each experiment, considering the corresponding value obtained for t_d. This equation showed good agreement with the fitted experimental data, with determination coefficients (R^2) above 0.98. It is important to mention that Eq. (9) was not used to represent the drying kinetics physically but only to obtain a more accurate prediction of t_d according to the experimental results.

$$X^*(t) = A\exp(-kt^n) \quad (9)$$

A 3^3 full-factorial design was used, with three replicates at the central point, considering three solids loads (26 g, 58 g, and 90 g, corresponding to bed heights of about 0.3 cm, 0.6 cm, and 0.9 cm, respectively), three air temperatures (50 °C, 70 °C, and 90 °C), and three airflow velocities (2.5 m/s, 3.5 m/s, and 4.5 m/s), resulting in 29 assays. The ranges of the variables were chosen according to the operational limits of the equipment, as well as to avoid particles falling through the solids support screen or being entrained away from the drying chamber.

The results were treated using the response surface technique, employing Statistica 7.0 software for the statistical analysis and mathematical modeling. Multiple regression of the data, using a significance level of 0.05, was used to quantify the effects of the variables, as well as their interactions and quadratic contributions. The independent variables were treated in their coded forms, as given by Eqs. (10),(11), and (12).

$$x_1 = \frac{m_p - 58}{32} \quad (10)$$

$$x_2 = \frac{T_f - 70}{20} \quad (11)$$

$$x_3 = u - 3.5 \quad (12)$$

An analysis of variance (ANOVA) was applied to evaluate the quality of the model fitted to the data.

F-statistic (ratio between two mean squares) was used to compare the variances in the hypothesis test [44]. The significance level was 0.05 for each hypothesis test.

The operating conditions that provided the lowest energy consumption and shorter drying times were subjected to an energy efficiency analysis.

RESULTS AND DISCUSSION

Drying kinetics experiments

The effects of air temperature, airflow velocity, and solids load on the drying process of iron ore fines are shown in Figure 5. The results for the other conditions presented the same behavior. As expected, the drying time decreased with the airflow velocity and temperature increase. An increase in the air temperature from 50 °C to 90 °C resulted in shorter residence times to reach the same moisture content due to the enhancement of the thermal capacity of the air and higher mass transfer rates. The initial period of the process was characterized by a substantial reduction of the moisture content, corresponding to the removal of free water from the material. On the other hand, the drying time increased when more solids were fed into the system. Souza Pinto *et al.* [27] reported a similar behavior for the effect of air temperature on the drying of iron ore with particle diameters less than 500 μm in an oven.

A thorough analysis of the effects of air temperature, airflow velocity, and solids load on drying time and specific energy consumption was performed by statistical analysis of the factorial design results.

Statistical analysis and response surface plots

Table 1 shows the solids loads (m_p, g) and the operational drying conditions, considering the air temperature (T_f, °C) and the airflow velocity (u_f, m/s), together with the corresponding responses for the drying time and the specific energy consumption, for each assay of the experimental design. The drying time and the SEC corresponded to the period required for the sample to achieve a moisture value of 0.05 kg water/kg dry solids. For example, when drying a solids load of 26 g at 50 °C and 2.5 m/s, the time required to decrease the moisture of the sample from its initial moisture content to a moisture content of 0.05 kg water/kg dry solids (t_d) was 79.2 s and the SEC was 18.8 MJ/kg.

The regressions resulted in residuals that were randomly distributed around the mean.

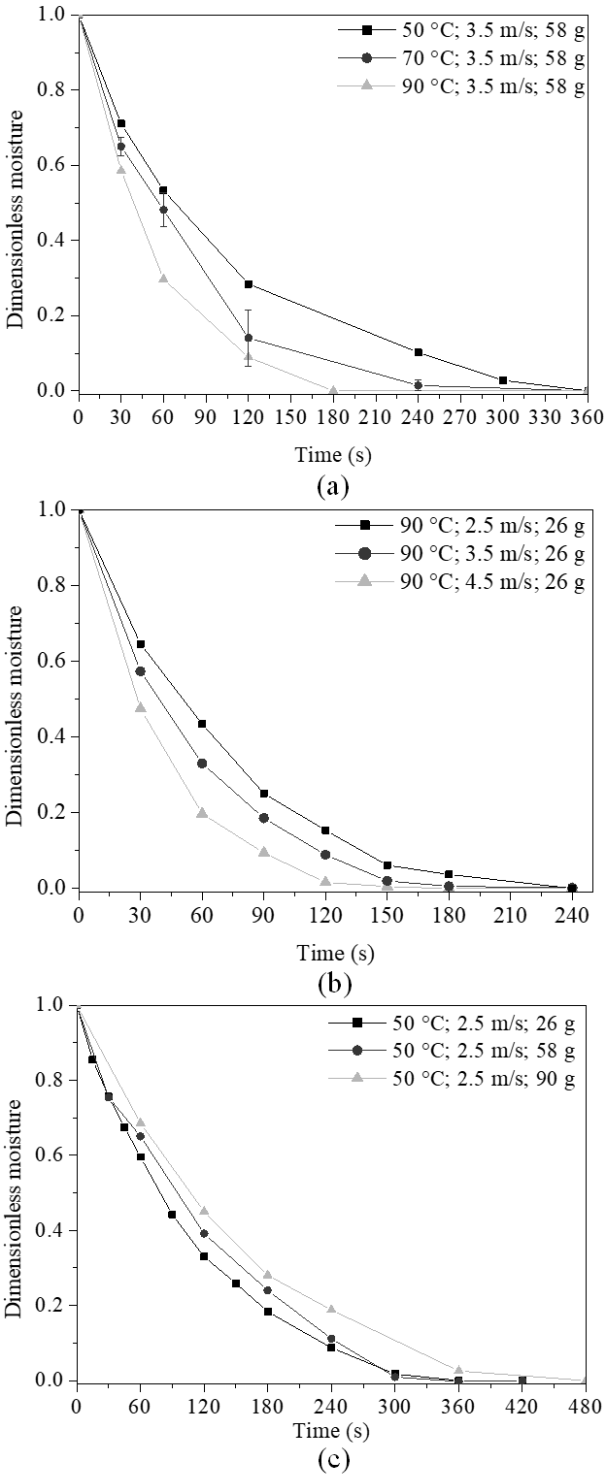

Figure 5. Drying kinetics curves for the convective drying of iron ore fines, showing the dimensionless moisture as a function of time for various experimental conditions: (a) comparing different inlet air temperatures, (b) airflow velocities, and (c) solids loads.

Effect of the independent variables on the drying time

The responses for the t_d (Table 1) ranged between 27.9 s and 105.6 s. Multiple regression of the experimental data resulted in the polynomial fit described by Eq. 13 for the drying time, with the

Table 1. Factorial design (3^3): settings and responses for the drying time and the specific energy consumption to a moisture content of 0.05 kg water/kg dry solids.

Independent variables			Responses	
m_p [g] (x_1)	T_f [°C] (x_2)	u [m/s] (x_3)	t_d (s)	E_s (MJ/kg)
26(-1)	50(-1)	2.5(-1)	79.2	18.8
26(-1)	70 (0)	2.5(-1)	54.5	21.9
26(-1)	90(+1)	2.5(-1)	45.4	24.9
26(-1)	50(-1)	3.5 (0)	59.0	19.7
26(-1)	70 (0)	3.5 (0)	42.2	23.8
26(-1)	90(+1)	3.5 (0)	34.4	26.4
26(-1)	50(-1)	4.5(+1)	51.7	22.1
26(-1)	70 (0)	4.5(+1)	29.7	21.5
26(-1)	90(+1)	4.5(+1)	27.9	27.5
58(0)	50(-1)	2.5(-1)	87.9	9.4
58(0)	70 (0)	2.5(-1)	55.1	9.9
58(0)	90(+1)	2.5(-1)	43.9	10.8
58(0)	50(-1)	3.5 (0)	64.2	9.6
58(0)	70 (0)	3.5 (0)	56.0	14.1
58(0)	70 (0)	3.5 (0)	47.6	12.0
58(0)	70 (0)	3.5 (0)	51.1	12.9
58(0)	90(+1)	3.5 (0)	29.7	10.2
58(0)	50(-1)	4.5(+1)	54.7	10.5
58(0)	70 (0)	4.5(+1)	37.7	12.2
58(0)	90(+1)	4.5(+1)	30.3	13.4
90(+1)	50(-1)	2.5(-1)	105.6	11.3
90(+1)	70 (0)	2.5(-1)	66.1	11.9
90(+1)	90(+1)	2.5(-1)	47.3	11.6
90(+1)	50(-1)	3.5 (0)	89.0	13.3
90(+1)	70 (0)	3.5 (0)	48.5	12.2
90(+1)	90(+1)	3.5 (0)	41.3	14.2
90(+1)	50(-1)	4.5(+1)	75.5	14.5
90(+1)	70 (0)	4.5(+1)	50.5	16.4
90(+1)	90(+1)	4.5(+1)	33.0	14.6

variables in coded form. Only the terms influencing the response within a 95% confidence interval are presented.

$$t_d = 48.9942 + 7.3695x_1 - 18.5336x_2 + 6.5715x_2^2 - 10.7689x_3 - 5.5254x_1x_2 + 3.7907x_2x_3 \quad (13)$$

The determination coefficient (R^2) for this empirical model was 0.958, indicating that Eq. 13 could explain 95.8% of the variability of the t_d responses. Statistical evaluation of the model obtained for t_d (Eq. 13) was performed using analysis of variance (ANOVA), as shown in Table 2. According to the literature [44], the calculated value of the F distribution for the regression should be about 3 times higher than the tabulated value for the model to be considered statistically significant. This requirement was fulfilled since $F_{calc(regression/residual)}$ = 33.1 $F_{tab(regression/residual)}$. Furthermore, the model showed no lack of fit ($F_{calc(lack\ of\ fit/pure\ error)} < F_{tab(lack\ of\ fit/pure\ error)}$). Therefore, the independent variables were sufficient to describe the behavior of t_d in the range studied.

There were significant effects of all the independent variables in isolated form and the quadratic term corresponding to air temperature. The independent variable T_f (x_2, coded) showed the greatest effect on t_d. In addition, interaction effects were identified between the variables solids load and air temperature and air temperature and air velocity. The significant interaction effects observed among all three variables highlighted the importance of evaluating them simultaneously when analyzing the iron ore drying time.

The response surfaces (Figure 6) showed that t_d decreased when lower solids loads, higher air temperatures, and higher airflow velocities were employed. These effects were physically coherent regarding the drying phenomena for the constant drying rate period.

Figure 6 could be used to investigate the interaction effects between the independent variables. Regarding the interaction of m_p and T_f, an increase of 42% in the drying time was calculated between the lower and upper level of m_p for the lowest air temperature. On the other hand, when the highest air temperature was used, a t_d increase of only 10% was observed, considering the same m_p levels. Therefore, the magnitude of the influence of the air temperature on t_d depended on the solids load in the bed. This behavior could be explained by considering the relation between the air temperature and the quantity of heat supplied to the sample per unit mass. When lower temperatures were used, an increase in solids load caused a decrease in heat per unit mass supplied to the sample. Consequently, lower drying rates and longer drying times occurred because less energy per unit mass was available to supply the latent heat required to evaporate the water. However, heat transfer was sufficient for higher temperatures to ensure high drying rates for the solids loads evaluated. Therefore, at this condition, the increase of the solids load did not substantially affect the supply of heat per unit mass to the sample, so the drying time was less pronounced.

Although the conditions that employed higher air temperatures and airflow velocities demanded more

Table 2. ANOVA for drying time for a final moisture content of 0.05 kg water/kg dry solid (t_d).

Source of variation	Sum of squares	Degrees of freedom	Mean of square	F_{calc}
Regression	10081.56	6	1680.26	84.44
Residual	437.76	22	19.90	
Lack of fit	402.34	20	20.12	1.14
Pure error	35.41	2	17.70	
Total	10519.32	28	375.69	

$F_{tab(regression/residual)}$ = 2.55; $F_{tab(lackoffit/pureerror)}$ = 19.44

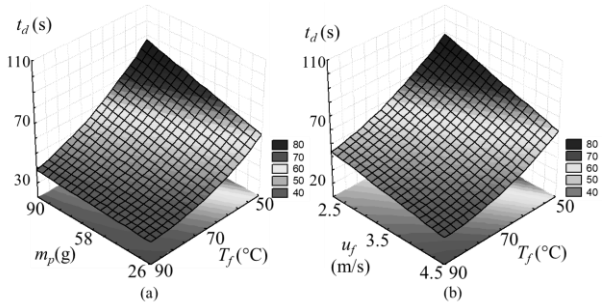

Figure 6. Response surfaces showing the drying time to a moisture content of 0.05 kg water/kg dry solid (t_d) as a function of the variables (a) air temperature and solids load and (b) air velocity and air temperature. In each case, the remaining variable was kept at the center level.

energy per unit of time to heat and blow the drying air, the value of t_d for these settings was substantially smaller. Therefore, the following analysis evaluated the SEC to understand the behaviour of the energy demand according to the process variables.

Effect of independent variables on energy consumption

E_s responses ranged between 9.4 MJ/kg and 27.5 MJ/kg (Table 1). Eq. (14) presents the multiple regression of the experimental data for E_s, disregarding the effects that were not statistically significant. A determination coefficient (R^2) of 0.959 was calculated for the polynomial quadratic model. Statistical evaluation of the model was performed using analysis of variance (ANOVA), as shown in Table 3. The model could be considered statistically significant since $F_{calc(regression/residual)} = 40.9\ F_{tab(regression/residual)}$. Furthermore, the model showed no lack of fit ($F_{calc(lack\ of\ fit/pure\ error)} < F_{tab(lack\ of\ fit/pure\ error)}$).

$$E_s = 11373.77 - 4815.89x_1 + 6779.86x_1^2 + 1354.58x_2 + 1239.56x_3 - 1339.24x_1x_2 \quad (14)$$

There were significant effects of all the variables in isolated form and the presence of a quadratic term for the solids load. There was also a significant interaction between the solids load and the air temperature. For the range of operating conditions evaluated, the independent variable m_p (x_1, coded) had the greatest influence on E_s, followed by air temperature and air velocity. Brito *et al.* [33] also found that the specific energy consumption was significantly affected by air temperature and solids load for convective drying of sorghum seeds.

Table 3. ANOVA for specific energy consumption for final moisture of 0.05 (E_s).

Source of variation	Sum of squares	Degrees of freedom	Mean of square	F_{calc}
Regression	815489765	5	163097953	108.035
Residual	34722496	23	1509673.7	
Lack of fit	32462494	21	1545833	1.36799
Pure error	2260002	2	1130001	
Total	850212261	28	30364724	

$F_{tab(regression/residual)} = 2.64$; $F_{tab(lackoffit/pureerror)} = 19.45$

Although the processes with high values of T_f and u_f consumed more energy, the drying time was substantially shorter under these conditions. For example, maintaining the higher load of solids and changing the temperature and air velocity levels from their lower to upper limits resulted in an approximately 69% reduction in the drying time and a 29% increase in E_s. Although the higher energy consumption is generally undesirable, this additional energy cost could be inevitable depending on the process demands or conditions (such as the solids' residence time in the equipment).

The response surfaces for E_s (Figure 7) showed that the energy consumption increased when higher air temperatures and airflow velocities were used. The quadratic behavior of the E_s response concerning the solids load indicated a point of minimum energy consumption at a specific m_p within the ranges of the variables analyzed. The energy consumption decreased as the solids load increased. This behavior was consistent because the energy consumption was inversely proportional to the solids load (Eq. 8). However, there was a limit to this trend since a further increase of the solids load led to less heat being absorbed per unit mass. Furthermore, a higher solids load implied a higher solids bed height, which increased the temperature and moisture gradients between the layers of agglomerates located at the bottom and the top of the sample. Consequently, the material heated up more slowly, and the evaporation rate decreased, leading to increased drying time and energy consumption. For these reasons, the E_s values declined to a minimum as m_p increased and then went back up. Therefore, a compromise between the solids load and the process conditions was required to minimize the energy consumption of the iron ore convective drying process.

Experimental optimization

An energy optimization analysis was performed, considering the drying air conditions that provided the shortest drying time within the ranges of the studied variables (T_f = 90 °C; u_f = 4.5 m/s). For these settings, the corresponding solids load value that minimized the

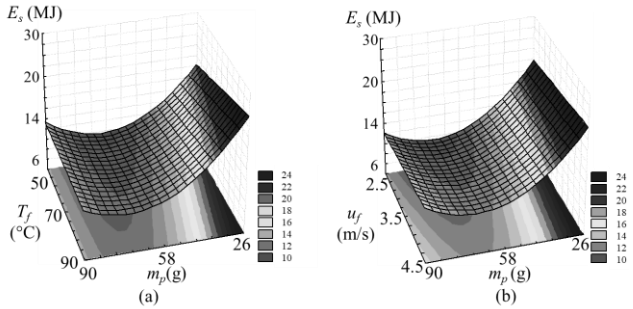

Figure 7. Response surfaces showing the specific energy consumption (E_s) as a function of the variables (a) air temperature and solids load and (b) air velocity and solids load, considering a final moisture content of 0.05 kg water/kg dry solid. In each case, the remaining variable was kept at the center level.

energy consumption was estimated using the regression equation for E_s (Eq. 14). As a result, a value of m_p of approximately 73 g (bed height of about 0.8 cm) was obtained, with estimated values of t_d (Eq. 13) and E_s (Eq. 14) of 30.9 s and 11.8 MJ/kg, respectively. New drying assays were performed in triplicate for this m_p value to validate the values predicted from the regression equations and determine the experimental results for t_d and E_s. As a result, a t_d value of 29.0±0.6 s was obtained, with E_s of 12.8±0.3 MJ/kg, the lowest E_s observed for these air conditions (T_f and u_f). Furthermore, deviations of 6.1% and 8.6% were calculated between the values estimated by Eqs. (13) and (14) and the experimental t_d and E_s results, respectively. Therefore, the assays performed under the optimal conditions confirmed the models' predictions for the evaluated experimental region within a significance level of 0.05.

Energy analysis

Figure 8 shows the curves for energy efficiency (filled symbols) and drying efficiency (open symbols), according to drying time, for different solids loads at a given air temperature and velocity. For all the conditions, the drying efficiency was higher than the energy efficiency because part of the sensible heat was used to heat the material [14]. However, the curves showed a steady decrease in the drying efficiency with time, up to approximately 100 s–120 s, after which the decrease was less pronounced. It could be explained by the fact that the removal of the remaining water in the final stages became increasingly difficult due to the lower gradients of water concentration and temperature between the drying air and the solids. Furthermore, the moisture content became close to equilibrium, and the process was limited by internal mass transfer mechanisms [14]. Given the moderate removal of moisture that is desired for iron ore fines (a final product moisture content of 0.05 kg water/kg dry solid was adopted here), this result provides further evidence that operation within the drying period limited by external moisture diffusion could provide substantial energy savings for the drying process [27].

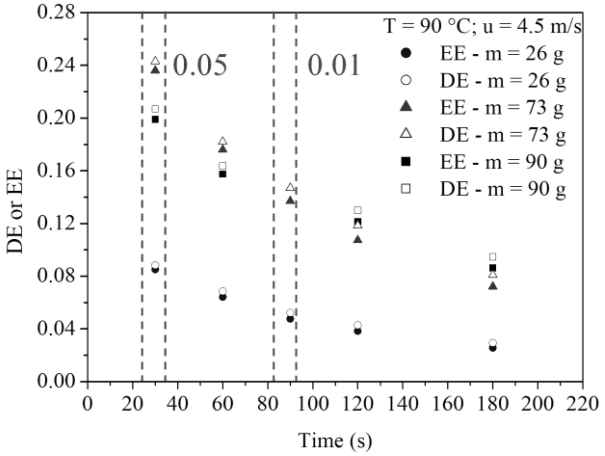

Figure 8. Drying and energy efficiencies for different solids loads as a function of time. The dashed lines indicate the approximate time intervals in which all the samples reached humidity values of 0.05 kg water/kg dry solid and 0.01 kg water/kg dry solid during drying.

The condition with the lowest mass showed the minimum DE and EE values. In convective drying processes, the attainment of high efficiency is hindered by the high amount of unsaturated air leaving the dryer, as well as by the short residence time of the air. Based on Eq. 6 and Eq. 7, increasing the quantity of water evaporated will increase the energy and drying efficiencies. Since the thermal energy supplied to the dryer was the same for all three conditions, the configurations with higher loads allowed higher saturation of the drying air, consequently increasing energy efficiency. On the other hand, the higher the solids load, the lower the quantity of heat transferred per unit mass of the sample, so the drying rate started to decrease when an excess of solids was fed to the system. Therefore, the mass of 73 g (bed height of about 0.8 cm) estimated by the response surface method represented the optimum value among the conditions analyzed.

The approach presented in this energy analysis provides a base for further investigation on the design of iron ore dryers, for example, when sizing conveyor dryers considering airflow conditions, product retention time, and bed height.

CONCLUSION

Statistical analysis of the drying results demonstrated that air temperature, airflow velocity, and solids load significantly affected the drying time and the specific energy consumption to a moisture content of

0.05 kg water/kg dry solid. The response surface method showed that a specific load of solids for each air condition could minimize the energy consumption for an iron ore drying process on a fixed bed. This finding means that a successive increase in the solids load decreases the energy consumption of the drying process only to a certain degree, after which the energy consumption rises. According to the optimization scheme of the experiments, when the highest values of air temperature (T_f = 90 °C) and air velocity (u_f= 4.5 m/s) were employed, the lowest energy consumption was obtained for a solids load of 73 g.

The results presented in this work show that efficient use of energy in drying operations of iron ore fines in fixed beds requires a compromise between the solids load, air temperature, and airflow velocity. Therefore, the approach presented here for identifying the optimum values of these variables should assist in designing and operating energy-efficient convective dryers for iron ore fines.

ACKNOWLEDGEMENT

This study was financed in part by the Coordenação de Aperfeiçoamento de Pessoal de Nível Superior - Brasil (CAPES) - Finance Code 001. In addition, this work was supported by CNPq- Brazil under Grant [142102/2019-9]; and Vale S.A. - Brazil.

NOTATION

c_p	Specific heat of air, kJ kg^{-1} K^{-1}
c_{ps}	Specific heat of solids, kJ kg^{-1} K^{-1}
DE	Drying efficiency
EE	Energy efficiency
ΔH_s	Latent heat of vaporization of hematite, kJ kg^{-1}
$\dot{m}$	Mass flow rate of air, kg s^{-1}
m_{ds}	Mass of dry solids, kg
m_p	Load of solids, g
m_{ws}	Mass of wet solids, kg
Q	Thermal energy supplied, kJ s^{-1}
Q_m	Energy required to heat the material, kJ
Q_w	Energy required to evaporate the water, kJ
E_s	Specific energy consumption for final moisture of 0.05 (dry basis), MJ kg^{-1}
t	Time, s
t_d	Drying time for a final moisture content of 0.05 (dry basis), s
T_a	Ambient temperature, °C
T_f	Drying air temperature, °C
u_f	Airflow velocity, m/s
x_1	Coded form of variable m_p
x_2	Coded form of variable T_f
x_3	Coded form of variable u_f
X^*	Dimensionless moisture
$\overline{X}$	Mean moisture in dry basis, kg kg^{-1}
X_i	Initial moisture in dry basis, kg kg^{-1}
X_{eq}	Moisture at dynamic equilibrium in dry basis, kg kg^{-1}

REFERENCES

[1] F.P. Van Der Meer, Miner. Eng. 73 (2015) 21–30. https://doi.org/10.1016/j.mineng.2014.12.018.

[2] A. Abazarpoor, M. Halali, R. Hejazi, M. Saghaeian, Miner. Process. Extr. Metall. 127 (2018) 40–48. https://doi.org/10.1080/03719553.2017.1284414.

[3] H.J. Haselhuhn, S.K. Kawatra, Miner. Process. Extr. Metall. Rev. 36 (2015) 370–376. https://doi.org/10.1080/08827508.2015.1004401.

[4] M.C. Munro, A. Mohajerani, Mar. Struct. 40 (2015) 193–224. https://doi.org/10.1016/j.marstruc.2014.11.004.

[5] International Maritime Organization (IMO), Amendments (05-19) to the International Maritime Solid Bulk Cargoes (IMSBC) Code (on 1 January 2021) (MSC101/24Add.3), London, (2019).

[6] D.D.C. Moreira, C.A.S. dos Santos, A.L.A. Mesquita, D.C. Moreira, Powder Technol. 373 (2020) 301–309. https://doi.org/10.1016/j.powtec.2020.06.052.

[7] R.F. Ferreira, T.M. Pereira, R.M.F. Lima, Powder Technol. 345 (2019) 329–337. https://doi.org/10.1016/j.powtec.2019.01.024.

[8] S.P. Suthers, V. Nunna, A. Tripathi, J. Douglas, S. Hapugoda, Trans. Inst. Min. Metall., Sect. C 123 (2014) 212–227. https://doi.org/10.1179/1743285514Y.0000000067.

[9] A.S. Patra, D. Makhija, A.K. Mukherjee, R. Tiwari, C.R. Sahoo, B.D. Mohanty, Powder Technol. 287 (2016) 43–50. https://doi.org/10.1016/j.powtec.2015.09.030.

[10] C.C. Mwaba, Miner. Eng. 4 (1991) 49–62. https://doi.org/10.1016/0892-6875(91)90118-F.

[11] J. Smith, C. Sheridan, L. van Dyk, S. Naik, N. Plint, H.D.G. Turrer, Miner. Eng. 115 (2018) 1–3. https://doi.org/10.1016/j.mineng.2017.10.011.

[12] B.L. Krasnyi, V.P. Tarasovskii, A.B. Krasnyi, Refract. Ind. Ceram. 50 (2009) 107–111. https://doi.org/10.1007/s11148-009-9156-1.

[13] M. Huttunen, L. Nygren, T. Kinnarinen, A. Häkkinen, T. Lindh, J. Ahola, V. Karvonen, Miner. Eng. 100 (2017) 144–154. https://doi.org/10.1016/j.mineng.2016.10.025.

[14] T. Kudra, Dry. Technol. 22 (2004) 917–932. https://doi.org/10.1081/DRT-120038572.

[15] T. Kudra, Dry. Technol. (2012) 1190–1198. https://doi.org/10.1080/07373937.2012.690803.

[16] A.S. Mujumdar, Handbook of Industrial Drying, 4th Ed., CRC Press, Boca Raton (2015), 861–866.

[17] A. Sass, Ind. Eng. Chem. Process Des. Dev. 7 (1968) 319–320. https://doi.org/10.1021/i260026a031.

[18] United States Geological Survey (USGS), Iron ore in May 2021, https://d9- wret.s3.us- west- 2.amazonaws.com/assets/palladium/production/s3fs-public/atoms/files/mis-202105-feore.pdf [accessed 6 September 2021].

[19] B.A. Chaedir, J.C. Kurnia, A.P. Sasmito, A.S. Mujumdar, Dry. Technol. 39 (2021) 1667–1684. https://doi.org/10.1080/07373937.2021.1907754.

[20] Z.H. Wu, Y.J. Hu, D.J. Lee, A.S. Mujumdar, Z.Y. Li, Dry. Technol. 28 (2010) 834–842. https://doi.org/10.1080/07373937.2010.490485.

[21] T. Tsukerman, C. Duchesne, D. Hodouin, Int. J. Miner. Process. 83 (2007) 99–115. https://doi.org/10.1016/j.minpro.2007.06.004.

[22] M. Athayde, M.C. Fonseca, B.M. Covcevich, Miner. Process. Extr. Metall. Rev. 39 (2018) 266–275. https://doi.org/10.1080/08827508.2017.1423295.

[23] A.L. Ljung, T.S. Lundström, B.D. Marjavaara,

K. Tano, Int. J. Heat Mass Transf. 54 (2011) 3882–3890. https://doi.org/10.1016/j.ijheatmasstransfer.2011.04.040.
[24] S. Tan, J. Peng, H. Shi, Dry. Technol. 34 (2016) 651–664. https://doi.org/10.1080/07373937.2015.1070357.
[25] J.X. Feng, Y. Zhang, H.W. Zheng, X.Y. Xie, C. Zhang, Int. J. Miner. Metall. Mater. 17 (2010) 535–540. https://doi.org/10.1007/s12613-010-0354-0.
[26] W. Namkung, M. Cho, Dry. Technol. 22 (2004) 877–891. https://doi.org/10.1081/DRT-120034268.
[27] T.C. Souza Pinto, A.S. Souza, J.N.M. Batista, A.M. Sarkis, L.S.L. Filho, T.F. Pádua, R. Béttega, Dry. Technol. 39 (2020) 1359–1370. https://doi.org/10.1080/07373937.2020.1747073.
[28] A. Okunola, T. Adekanye, E. Idahosa, Res. Agric. Eng. 67 (2021) 8–16. https://doi.org/10.17221/48/2020-RAE.
[29] N. Zhang, L. Shi, H. Qi, Y. Xie, L. Cai, Dry. Technol. 34 (2016) 161–166. https://doi.org/10.1080/07373937.2015.1012677.
[30] J.Q. Xu, R.P. Zou, A.B. Yu, Powder Technol. 169 (2006) 99–107. https://doi.org/10.1016/j.powtec.2006.08.004.
[31] AOAC, Official Methods of Analysis of the Association of Official Analytical Chemists, 17th ed., AOAC International, Maryland (2002).
[32] G. Albini, F.B. Freire, J.T. Freire, Chem. Eng. Process. - Process Intensif. 134 (2018) 97–104. https://doi.org/10.1016/j.cep.2018.11.001.
[33] R.C. de Brito, T.F. de Pádua, J.T. Freire, R. Béttega, Chem. Eng. Process. - Process Intensif. 117 (2017) 95–105. https://doi.org/10.1016/j.cep.2017.03.021.
[34] M.G.A. Vieira, L. Estrella, S.C.S. Rocha, Dry. Technol. 25 (2007) 1639–1648. https://doi.org/10.1080/07373930701590806.
[35] A.E. Takegoshi, Y. Hirasawa, S. Imura, T. Shimazaki, Int. J. Thermophys. 5 (1984) 219–228. https://doi.org/10.1007/BF00505502.
[36] J. Jang, H. Arastoopour, Powder Technol. 263 (2014) 14–25. https://doi.org/10.1016/j.powtec.2014.04.054.
[37] T. Kudra, Chem. Process Eng. 19 (1998) 163–172. ISSN 0208-6425.
[38] E. Holtz, L. Ahrné, T.H. Karlsson, M. Rittenauer, A. Rasmuson, Dry. Technol. 27 (2009) 173–185. https://doi.org/10.1080/07373930802603334.
[39] P. Karimi, H. Abdollahi, N. Aslan, M. Noaparast, S.Z. Shafaei, Miner. Process. Extr. Metall. Rev. 32 (2011) 1–16. https://doi.org/10.1080/08827508.2010.508828.
[40] Z. Cai, Y. Feng, H. Li, X. Liu, Miner. Process. Extr. Metall. Rev. 36 (2015) 1–6. https://doi.org/10.1080/08827508.2012.762915.
[41] K. Meyer, Pelletizing of Iron Ores, Springer-Verlag, Heidelberg (1980).
[42] A. Midilli, H. Kucuk, Z. Yapar, Dry. Technol. 20 (2002) 1503–1513. https://doi.org/10.1081/DRT-120005864.
[43] E.M. Silva, J.S. Da Silva, R.S. Pena, H. Rogez, Food Bioprod. Process. 89 (2011) 39–46. https://doi.org/10.1016/j.fbp.2010.03.004.
[44] G.E.P. Box, J.S. Hunter, W.G. Hunter, Statistics for Experimenters: Design, Innovation and Discovery, 2nd Ed., John Wiley & Sons, New Jersey (2005). ISBN: 978-0-471-71813-0.

AMARÍLIS SEVERINO E SOUZA[1]

THIAGO CÉSAR DE SOUZA PINTO[2]

ALFREDO MOISÉS SARKIS[3]

THIAGO FAGGION DE PÁDUA[1]

RODRIGO BÉTTEGA[1]

[1]Federal University of São Carlos, Department of Chemical Engineering, Drying Center of Pastes, Suspensions, and Seeds, São Carlos, SP, Brazil

[2]Mineral Development Center – CDM/Vale, Santa Luzia, MG, Brazil

[3]Instituto Tecnológico Vale – ITV, Santa Luzia, MG, Brazil

NAUČNI RAD

ENERGETSKA ANALIZA KONVEKTIVNOG SUŠENJA FINE GVOZDENE RUDE

Operacije sušenja u postrojenjima za preradu rude gvožđa imaju posebno veliku potražnju za energijom zbog velikog protoka čvrstog materijala koji se koristi u ovoj industriji. 3^3 potpuni faktorijalni plan je primenjen za istraživanje uticaja temperature vazduha, brzine protoka vazduha i količine čvrstog materijala na vreme sušenja i specifičnu potrošnju energije konvektivnog sušenja fine rude gvožđa u nepokretnom sloju. Rezultati su pokazali da je svaki uslov vazduha za sušenje bio povezan sa optimalnom količinom čvrstog materijala koje je minimiziralo specifičnu potrošnju energije . Količina od 73 g (visina sloja od oko 0,8 cm) je identifikovana i potvrđena kao optimalna u pogledu potrošnje energije za konfiguraciju sa najvišom temperaturom (90 °C) i brzinom protoka vazduha (4,5 m/s). Pri ovom uslovu vreme sušenja je 29 s i odgovarajućom specifičnom potrošnjom energije od 12,8 MJ/kg, pri čemu se vlaga smanjuje sa 0,11 kg vode/kg suve čvrste materije na 0,05 kg vode/kg suve čvrste materije. Identifikovanje optimalnih vrednosti za procesne promenljive trebalo bi da pomogne u projektovanju i radu energetski efikasnih konvektivnih sušara za fine rude gvožđe.

Ključne reči: aglomerati gvozdene rude, granica prenosive vlage, potrošnja energije, efikasnost sušenja, peletna hrana.